Astron. Astrophys. 322, 391–399 (1997)

ASTRONOMY
AND
ASTROPHYSICS

On the ionization of the diffuse ionized gas: spectroscopy of NGC 2188⋆

H. Domgörgen[1] **and R.-J. Dettmar**[2]

[1] Sternwarte der Universität Bonn, Auf dem Hügel 71, D-53121 Bonn, Germany
[2] Astronomisches Institut der Ruhr-Universität Bochum, Universitätsstr. 150, D-44780 Bochum, Germany

Received 2 September 1996 / Accepted 2 December 1996

Abstract. NGC 2188 is a highly inclined irregular galaxy which shows spectacular filaments of ionized gas emerging from an HII region complex into the halo of the galaxy. Here we present Hα imaging and optical spectroscopy of NGC 2188. Since the galaxy is low in metallicity and dust poor, the spectroscopic observations open up a parameter range for the extraplanar DIG which is not yet explored. Using empirical diagnostic diagrams we find that the ionized gas above the plane is most likely photoionized. Differences in line ratios between the DIG in spiral galaxies and in NGC 2188 can fully be explained by differences in metallicities. We argue that dust is not of high importance in altering the line ratios measured for the DIG either by scattering or photoelectric heating.

Key words: galaxies: halos – galaxies: individual: NGC 2188 – galaxies: ISM – galaxies: irregular

1. Introduction

The ionization of the diffuse ionized gas (DIG) or warm ionized medium (WIM) observed outside of classical HII regions is a topic strongly under debate. Estimates for the Milky Way show that no source but the Ly continuum radiation of young OB stars can provide enough power to maintain its ionization (Reynolds 1984). However, neutral hydrogen seems to be ubiquitous and the optical depth for Lyman continuum photons in a neutral medium is large.

One important tool to clarify the issue is optical spectroscopy. Measuring line ratios of optical emission lines allows the investigation of the ionization of the DIG. By subsequent comparison with theoretically expected line ratios, properties of the ionizing sources can be determined.

Ratios of nebular emission lines at various wavelengths have been determined from Fabry-Perot measurements of the DIG in the Galaxy. These show that the spectrum of the DIG is different from that of classical HII regions: [SII]/Hα and [NII]/Hα are stronger (Reynolds 1985a, b), [OIII] λ5007 Å is weak and upper limits could be determined for [OI] λ6300 Å (Reynolds 1989) and HeI λ5876 Å (Reynolds & Tufte 1995). Additionally, spectroscopy of the extraplanar DIG of NGC 891 (Dettmar & Schulz 1992) and NGC 4631 (Golla et al. 1995) shows that both [NII] λ6584/Hα and [SII] λ6717/Hα increase with vertical distance from the plane and reach values a factor of two higher than those for the galactic DIG.

Although different from an HII region spectrum, many of these features can be accounted for by low-excitation low-density photoionization model calculations (Domgörgen & Mathis 1994). Some questions, however, remain open. The non-detection of HeI emission implies a very soft ionizing spectrum similar to that of late O and early B stars. These stars contribute only 22% to the ionizing radiation (Abbott 1982). Moreover, the models cannot account for the highest [NII] λ6584/Hα that has been observed in NGC 891. Therefore it has been suggested that photoelectric heating by dust (Reynolds & Cox 1992) might play an important role for the energy balance of the DIG.

In order to look further into these problems we performed Hα imaging and long-slit spectroscopy of the irregular galaxy NGC 2188. Its axial ratio of 0.23 implies a high inclination of $\sim 87°$ (Tully 1988). Since NGC 2188 is a metal-poor system (Stasinska et al. 1986), spectroscopy of its filamentary gas allows us to study the ionization state of extraplanar ionized gas under conditions different from those of spiral galaxies. Additionally, the high gas to dust ratio in dwarf irregular galaxies allows for an indirect test of the importance of dust for altering the spectrum of the DIG. In contrast to former observations of extraplanar DIG in galaxies, the spectroscopy presented here covers the whole wavelength range from 3500 to 7000 Å and some line ratios for extraplanar ionized features are measured for the first time.

2. Observations and data reduction

2.1. Narrow band Hα imaging

Hα images of NGC 2188 were obtained in Feb. 1993 with the ESO 2.2m telescope on La Silla, using EFOSC 2 (Melnick et

Send offprint requests to: H. Domgörgen

⋆ Based on observations obtained at ESO/La Silla (Chile)

al. 1989) with a 1024 × 1024 pixel Thompson CCD chip. The spatial scale is 0.″34/pixel; the seeing during our observations was $\simeq$ 0.″9, giving a linear resolution of 34 pc at a distance of 7.9 Mpc for NGC 2188 (Tully 1988). The integration times were 2 × 30 min with the Hα filter # 694, which has a $FWHM$ of 61 Å and a central wavelength of $\lambda_\circ$ = 6557 Å, and 10 min with Gunn r.

The data reduction was performed using the IRAF software package. Bias and dark were subtracted and sensitivity variations were removed using dome flatfields. We performed the continuum subtraction using the scaled R-band image (e.g., Dettmar 1990).

Lauberts & Valentijn (1989) measured an R-band magnitude of m_R = 11.45 for NGC 2188 in a 26″ aperture. This photometry and the fundamental calibration of αLyr by Tüg et al. (1977) were used to flux calibrate the image. At the wavelength of the redshifted [NII] λ6583 line, the sensitivity of the Hα filter is reduced by $\sim$ 20%. We know from the spectroscopic data (see below) that on average [NII] λ6583/Hα $\sim$ 0.15. The [NII] emission line then contributes $\sim$ 10% to the emission in the Hα image. To obtain the Hα surface brightness we subtract this estimated contribution. The sensitivity of the resulting map at a 1 σ level of the sky background is 1.6×10^{-18} erg s^{-1} cm^{-2} pix^{-1}. This corresponds to an emission measure (EM) of 7 cm^{-6} pc at an assumed electron temperature of 10^4 K.

2.2. Long-slit spectroscopy

Optical spectra at several positions perpendicular and parallel to the major axis of NGC 2188 were obtained with the B&C spectrograph at the 1.52m ESO telescope on La Silla (Oliveira 1994) in Jan. 1995. The detector was a FA 2048L front side illuminated and UV coated CCD with 2048×2048 pixels and a pixel size of 15 μm. The spatial scale is 0.″82/pixel. We used grating # 23 providing a dispersion of 126.2 Å/mm to cover a wavelength range from $\sim$ 3500 Å to $\sim$ 7500 Å. The resolution is 4 Å.

In Fig. 1 we show the slit positions for the spectroscopy superimposed on an Hα image of NGC 2188. In order to investigate the nature of the filamentary emission in NGC 2188 all spectra perpendicular to the plane were obtained for the southern emission line region of NGC 2188. In the following we refer to the northern-most slit position as slit position A, to the southern-most as position E.

The data reduction was performed using the MIDAS software package. The data were bias subtracted and small scale sensitivity variations were removed using dome flat fields. No significant fringing was observed. We corrected for extinction assuming the atmospheric extinction curve for La Silla measured by Tüg (1977). Observations of the standard stars EG 76 and Hiltner 600 which we obtained at the beginning and the end of each observing night were used to determine the response curve of the system. The slit length of 4′ provided simultaneous on and off source observations which allowed an accurate subtraction of the night sky spectrum.

3. Analysis

The long-slit spectra allow us to study the variation of the emission line intensities and their ratios along the slit. Emission of the strong nebular emission lines, i.e. [OII] λ3727 Å, Hβ, [OIII] λ5007 Å, Hα, [NII] λ6584 Å, and [SII] λ6717 Å are present in the spectra and can be measured for the bright HII regions as well as for the fainter filamentary gas. Additionally, emission of many weaker lines can be detected in regions of high surface brightness. In order to increase the signal to noise of the data we averaged the spectra over 9 pixels along the spatial direction. Then the ratios of various emission lines were measured for each position along the slit.

The Balmer emission lines for extragalactic objects are affected by underlying stellar absorption. The strength of the absorption depends on the stellar population in the line emitting region. Detailed studies of giant extragalactic HII regions show that for these objects the absorption equivalent width is typically 2 Å (e.g. Shields & Searle 1978; Skillman 1985). We corrected the Balmer emission for this value. The absorption equivalent width might in fact be different for the HII regions and the filamentary gas. Therefore we will also present the uncorrected data to demonstrate the possible influence of this effect.

In Sect. 5.2 we will compare the emission line ratios obtained with the empirical diagnostic diagrams by Baldwin et al. (1981). In order to avoid showing redundant data points we added the emission along the slit for subsections representing gas of different surface brightness (e.g. an HII region or a filament). For the low surface brightness emission the number of rows added was determined so that the signal to noise in the most important emission lines was sufficiently high and simultaneously a minimum number of rows was summed. The HII region spectra were corrected for 2 Å equivalent width absorption in the Balmer lines. For the faint emission line gas the Balmer lines in the blue, i.e. Hγ and Hδ, are too weak to show emission and we can give an upper limit to the Balmer absorption. A mean value of 1 Å was found and was corrected for.

Most of the line ratios under consideration here are intensity ratios of emission lines that are close to each other in wavelength. Consequently they are negligibly affected by differential extinction. This is not true for all line ratios involving [OII] λ3727 Å. We calculated the absorption corrected Balmer line ratio in order to derive the logarithmic reddening correction at Hβ, c(Hβ), which was then used to determine reddening corrected [OII] line ratios. An intrinsic Balmer line ratio for an electron temperature of 10000 K (Hα/Hβ = 2.85 as given by Brocklehurst (1971)) was assumed.

4. Results

4.1. Hα properties of NGC 2188

Fig. 1 shows the continuum subtracted Hα+[NII] image of NGC 2188. From the calibration of the Hα image we calculate a total flux of NGC 2188 in the Hα line of $F_{\rm H\alpha}$ = 1.6×10^{-12} erg cm^{-2} s^{-1}. This flux corresponds to a total Hα luminosity of $L_{\rm H\alpha}$= 1.1×10^{40} erg s^{-1} at a distance of 7.9 Mpc,

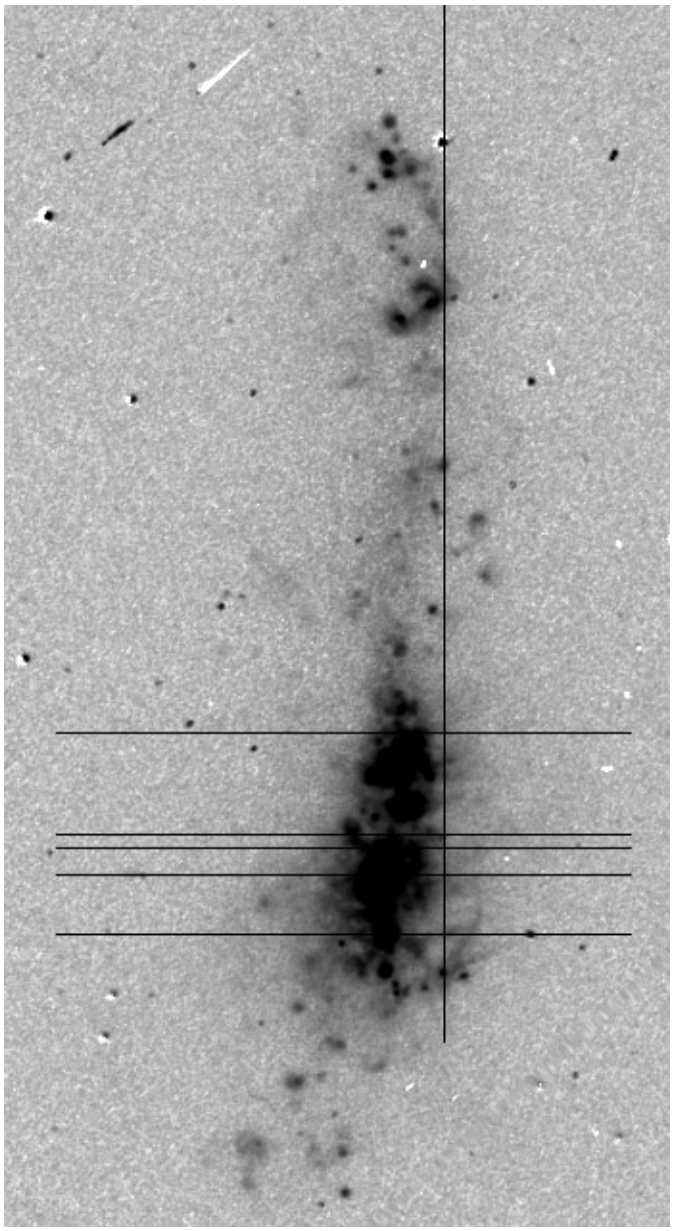

Fig. 1. Hα+[NII] emission line image of NGC 2188. The intensity is scaled logarithmically to show faint structures more clearly. Positions for which we obtained spectroscopy are indicated. North is up, east is left. The field of view is $2\farcm0 \times 3\farcm6$.

roughly a factor of 3 lower than the total Hα luminosity of the LMC.

80% of the Hα flux of NGC 2188 is coming from an HII region complex in the southern part of the galaxy. This complex extends ~ 2 kpc along the major axis of NGC 2188. It can be resolved into an agglomeration of ~ 15 smaller HII regions which are embedded into Hα emission of lower surface brightness. Since the inclination of NGC 2188 is 87°, the distribution of these HII region knots basically determines the thickness of the plane.

Probably the most spectacular features on the Hα image are the filaments of ionized gas that extend from the southern starforming region perpendicular to the plane of the galaxy. Some of these features are several hundred parsecs long. They typically have $EM \sim 100\,\mathrm{cm}^{-6}$ pc.

The whole southern complex is surrounded by Hα emitting gas of even lower surface brightness ($EM \sim 30\,\mathrm{cm}^{-6}$ pc). Such emission is also present in the northern disk. Ferguson et al. (1996) investigated the diffuse Hα emitting gas in the two spiral galaxies NGC 247 and NGC 7793. In order to separate the diffuse emission from the emission of classical HII regions they applied a cut-off criterion in surface brightness defining the emission with $EM < 80\,\mathrm{cm}^{-6}$ pc as diffuse. We apply the same cut-off to our data in order to estimate the fraction of Hα emission residing in the low surface brightness component of NGC 2188. The flux we measure for this diffuse Hα emitting component is 3.5×10^{-13} erg cm^{-2} s^{-1}. Thus 24% of the Hα emitting gas is truly diffuse. This fraction is only a lower limit since much DIG, in particular in the southern half of NGC 2188, might be superimposed on HII regions which is also indicated by the fact that a reasonable fraction of the diffuse emission (44%) comes from the northern part of the galaxy where also emission from the disk contributes.

$L_{\mathrm{H}\alpha}$ can be used to estimate the current star formation rate (SFR) of NGC 2188. Following Gallagher & Hunter (1987) $\dot{M} = 6.6 \times 10^{-42} \eta^{-1} L_{\mathrm{H}\alpha}\,\mathrm{M}_\odot\,\mathrm{yr}^{-1} = 0.11\ \mathrm{M}_\odot\,\mathrm{yr}^{-1}$. A Salpeter stellar mass function, an upper mass limit of $100\,\mathrm{M}_\odot$, and a lower mass cut-off of $10\,\mathrm{M}_\odot$ is assumed. The parameter η, an efficiency factor that accounts for dust absorption of Lyman continuum photons, is assumed to be 2/3 (Gallagher et al. 1984). This value for the SFR is a lower limit since we did not correct $L_{\mathrm{H}\alpha}$ for interstellar extinction although NGC 2188 is an edge-on system. Additionally, stellar Hα absorption lines have not been taken into account.

Another estimate of the current SFR comes from the IR luminosity. The *IRAS point source catalogue* lists $f_{60} = 2$ Jy and $f_{100} = 4.65$ Jy. We use the definition $L_{\mathrm{IR}} = 2.3 \times 10^{39} D^2(\mathrm{Mpc})[2.68 f_{60} + f_{100}]$ erg s^{-1} (Lonsdale et al. 1985) and get $L_{\mathrm{IR}} = 1.42 \times 10^{42}$ erg s^{-1}. Using similar assumptions as above $\dot{M} = 6.6 \times 10^{-44} \beta^{-1} L_{\mathrm{IR}}\,\mathrm{M}_\odot\,\mathrm{yr}^{-1}$, where β again is an efficiency factor with a value ~ 0.5 (Gallagher & Hunter 1987). We then calculate $\dot{M} = 0.19\,\mathrm{M}_\odot\,\mathrm{yr}^{-1}$. Considering the *many* uncertainties in these estimates the two SFRs agree fairly well. Therefore $L_{\mathrm{H}\alpha}$ is a good measure for the SFR, which means that NGC 2188 is a transparent system in spite of its high inclination.

The importance of dust in NGC 2188 can also be evaluated by the dust-to-HI gas mass ratio. Hunter et al. (1989) determined this ratio for a large sample of irregular and spiral galaxies using the *IRAS* flux to estimate the dust mass, M_{D}. M_{D} thus is only a formal number since it refers to the warm dust that *IRAS* detects. For reasons of comparison we calculate M_{D} following their arguments. M_{D} is calculated from its dependence on f_{60} and T_{D} for a silicate model. The *IRAS* flux at 60 and 100 μm yields $T_{\mathrm{D}} \sim 40$ K resulting in $M_{\mathrm{D}} = 1.2 \times 10^4\,\mathrm{M}_\odot$. Hunter et al. claim that for a graphite model M_{D} is approximately half of that. The HI mass of NGC 2188 is $3 \times 10^8\,\mathrm{M}_\odot$ (Domgörgen et al. 1996). The dust-

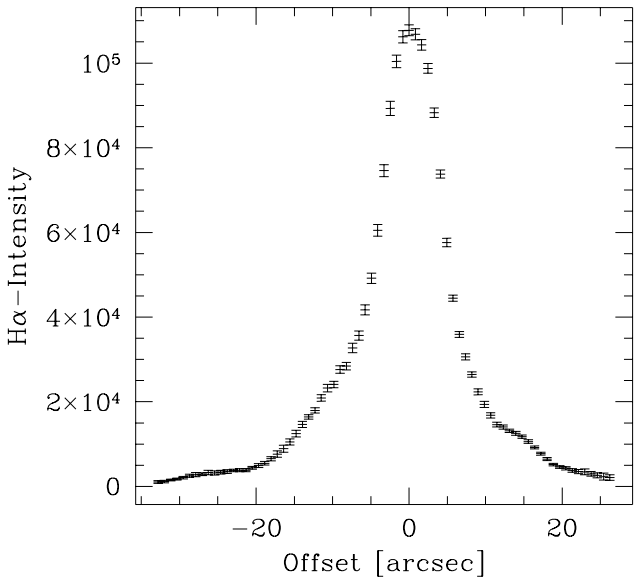

Fig. 2. Hα emission profile along slit position E. The intensity is given in arbitrary units.

to-HI mass ratio of NGC 2188 is then 2.3×10^{-4}, typical for the sample of irregular galaxies that has been investigated by Hunter et al. (1989; their Fig. 9) and considerably smaller than the dust-to-HI mass ratios of the spiral galaxy comparison sample. From this we conclude that NGC 2188 is a dust-poor system. It has to be pointed out though that the absolute dust-to-HI mass ratio is uncertain. Using the approach of Thronson & Telesco (1986) we find $M_{\rm D}$ to be a factor of 4.5 higher. Additionally, 30% of the HI emission of NGC 2188 comes from regions outside the stellar disk which might not contribute to the dust emission.

4.2. Variations of line ratios

The line ratios, their range, and general trends in their variation are similar for the five slit positions perpendicular to the plane of NGC 2188. As an example we will now discuss the results for slit position E in detail.

The Hα intensity along slit position E is shown in Fig. 2. The central intensity peak is defined as positional zero point and positive offsets correspond to positions west of the galaxy. Morphological features in the Hα image can easily be seen as emission features in the spectrum. The Hα intensity along slit position E is characterized by a strong peak corresponding to a bright HII region in the disk of NGC 2188 and broad wings. The intensity decreases steeply down to roughly 25% of the peak intensity from which point it falls more slowly. The broad wing to the west of the HII region peak is due to the two most prominent Hα filaments seen in NGC 2188 (see Fig. 1). One of them extends perpendicular to the plane into the halo. The second has a length of $\sim$ 500 pc and is the largest filamentary feature. Starting from some small HII regions in the southern most part of NGC 2188 this feature runs nearly parallel to the disk. To the east of the peak the Hα emission is a mixture of extended HII region envelope and filamentary emission. At offset positions of $\pm 20''$ the intensity has dropped to 5% of the maximum. Such low intensity corresponds to the diffuse non-filamentary Hα emission. Ionized gas can be traced nearly along $60''$ or 2.3 kpc perpendicular to the plane of NGC 2188.

Fig. 3a-d present the emission line ratios for [NII] λ6584/Hα, [SII] λ6717/Hα, [OIII] λ5007/Hβ, and [OII]/[OIII] for slit position E. Since most of the nebular emission lines are fainter than Hα or lie in less favorable parts of the optical spectrum, reliable line ratios could only be determined for $40''$ along the slit approximately centered around the HII region peak. [NII] λ6584/Hα, [SII] λ6717/Hα, and [OII]/[OIII] vary similarly: they show a minimum at the central HII region peak and increase with increasing offset position. The increase is larger for positive than for negative offsets. Two minima in the intensity ratios can be noticed at $\sim \pm 17''$. The minimum at $+17''$ can be attributed to the prominent filamentary emission. No particular morphological feature can be found to correspond to the minimum in the east. In contrast to the line ratios of the low ionization stages, [OIII] λ5007/Hβ is strong for the region with large Hα intensity and decreases with offset from the HII region emission peak. There is no pronounced difference between the variation of this intensity ratio west and east of the HII region peak.

It is a general result that the intensity ratios of the low ionization stages show a minimum for regions of high Hα intensity and increase with offset from the central HII region peak, i.e. decreasing surface brightness. The largest emission line ratios are usually measured at positions where the intensity is just above the detection limit. [OIII] λ5007/Hβ shows the opposite trend. The results for all slit positions are summarized in Table 1. The minimum for the HII region emission and the maximum for the filamentary emission is listed for the low ionization stages and vice versa for [OIII] λ5007/Hβ. This allows us to present the complete range of line ratios. Note that the absolute values for [OIII] λ5007/Hβ are higher for slit position E than for any of the other positions.

We also measured the intensity ratios for one slit position along the major axis in the disk of NGC 2188. Since $EM < 100\,{\rm cm}^{-6}$ pc for many regions in the northern part of NGC 2188 line ratios anywhere along the slit could only be studied for those emission lines in the most favorable part of the spectrum, i.e. Hα, [NII], and [SII]. The intensity ratios vary with surface brightness as described above for slit positions perpendicular to the plane. This is shown in Fig. 4 where we plot [SII] λ6717/Hα along with the Hα intensity: each Hα intensity maximum is accompanied by a minimum in [SII] λ6717/Hα. Also the absolute values of the line ratios are similar. We find [SII] λ6717/H$\alpha \sim 0.15$ and 0.45 for HII regions and the ionized gas respectively, and [NII] λ6584/H$\alpha \sim 0.1$ and 0.2.

A critical measurement for the hardness of the ionizing radiation field is the HeI λ5876/Hβ intensity ratio from which it is possible to calculate the ratio of He to H ionizing photons. Only upper limits could be determined for HeI λ5876/Hβ of the ionized gas outside of HII region emission line peaks. This is due to the limited sensitivity of the data and the presence of a nightsky emission line of Na I at the redshifted wavelength of

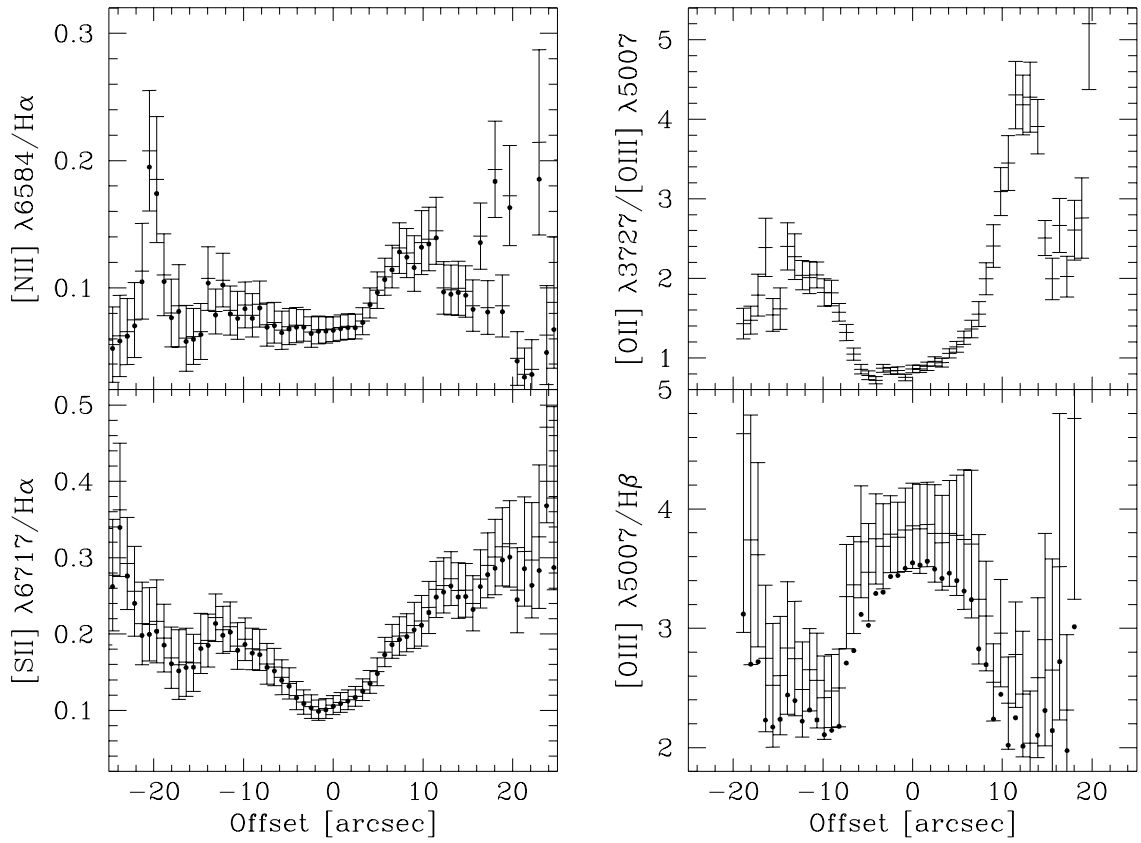

Fig. 3. The intensity ratios measured are plotted against position along the slit. An offset position of 0″ corresponds to the peak in the Hα emission. Positive offsets are measured to the west of the galaxy. Filled circles denote emission line ratios corrected for 2 Å equivalent width stellar absorption in the Balmer lines.

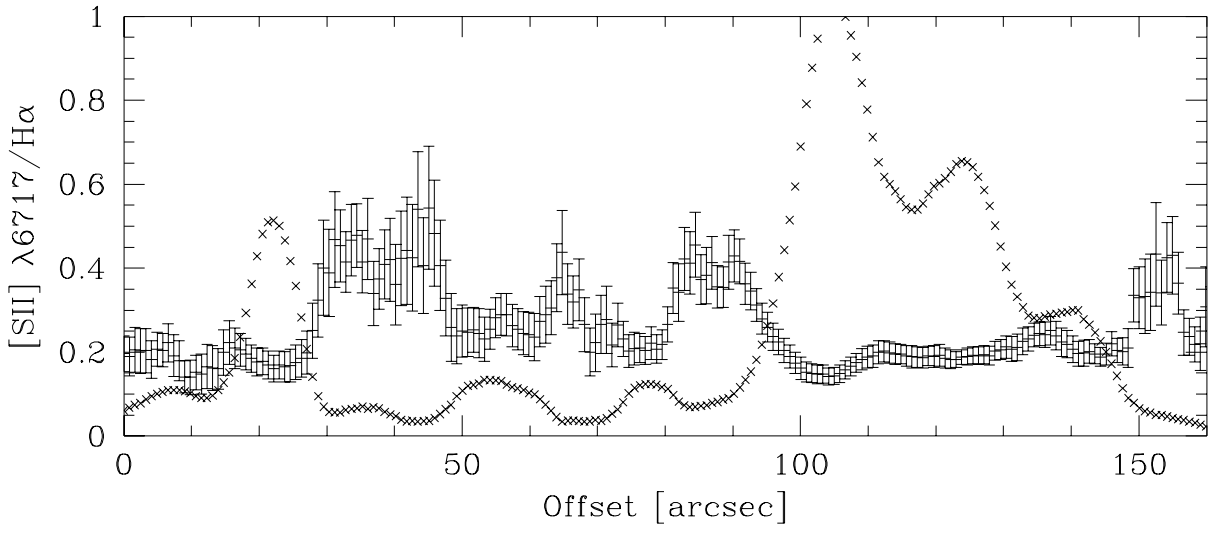

Fig. 4. The [SII] λ6717/Hα emission line ratio along the slit position parallel to the major axis is shown together with the scaled Hα intensity (crosses) is shown.

Table 1. Emission line ratios in NGC 2188

Slit Position	[SII] λ6717/Hα		[NII] λ6584/Hα		[OII]/[OIII]		[OIII] λ5007/Hβ	
	HII region	filaments	HII region	filaments	HII region	filaments	HII region	filaments
Minor A	0.11 ± 0.01	0.54 ± 0.10	0.08 ± 0.01	0.25 ± 0.06	1.03 ± 0.06	5.0 ± 0.7	3.2 ± 0.2	1.0 ± 0.3
Minor B	0.10 ± 0.02	0.32 ± 0.06	0.08 ± 0.01	0.20 ± 0.04	1.2 ± 0.1	8.0 ± 2.0	2.8 ± 0.1	0.9 ± 0.2
Minor C	0.11 ± 0.01	0.47 ± 0.17	0.07 ± 0.01	0.21 ± 0.06	1.0 ± 0.15	3.1 ± 0.3	2.9 ± 0.2	1.0 ± 0.2
Minor D	0.13 ± 0.02	0.36 ± 0.12	0.08 ± 0.01	0.16 ± 0.03	1.5 ± 0.1	4.8 ± 0.9	2.4 ± 0.3	1.1 ± 0.4
Minor E	0.10 ± 0.01	0.30 ± 0.05	0.06 ± 0.01	0.14 ± 0.03	0.86 ± 0.08	5.3 ± 0.4	3.5 ± 0.4	2.2 ± 0.4
Mean	0.11 ± 0.01	0.40 ± 0.10	0.07 ± 0.01	0.19 ± 0.04	1.12 ± 0.25	5.2 ± 1.8	3.0 ± 0.4	1.2 ± 0.5

HeI λ5876. All upper limits are ≥ 0.08 which corresponds to upper limits on He^+/H^+ that are larger than 0.6 He/H.

No systematic variations are found for the reddening. A mean value of $E(B-V) = 0.07$ as determined from Hα/Hβ is measured for the HII region peaks. This indicates that NGC 2188 is indeed a low-metallicity dust-poor environment. Spectrophotometry of an HII region in the southern part of NGC 2188 has also been presented by Stasinska et al.(1986). Their relative line intensities are in good agreement with our results and most of the differences can easily be accounted for by differences in slit positions.

5. Discussion

5.1. The nature of the extra-HII region gas in NGC 2188

The filamentary Hα emitting gas emerging from the southern HII region agglomeration in NGC 2188 is morphologically similar to the extraplanar diffuse ionized features in the lower halo of the edge-on spiral galaxy NGC 891. In both galaxies filaments extend from a starforming complex perpendicular to the disk several hundred parsec into the halo of the galaxy. Also the surface brightness of the features is comparable. From Fig. 3 in Dettmar (1990) we find that the EM of the Hα emitting gas in NGC 891 has dropped to 100 cm^{-6} pc, i.e. is comparable to the faint emission line filaments in NGC 2188, at $z \sim 600$ pc above the midplane.

There is increasing evidence that the existence of DIG is correlated with star formation, and NGC 2188 is yet another example supporting this idea. Ferguson et al. (1996) investigated the radial and azimuthal intensity distribution of the DIG in NGC 247 and NGC 7793 and found a strong correlation with bright HII regions. The Hα data of NGC 2188 confirm this result: prominent ionized filamentary features are present only in the vicinity of the southern HII region complex whereas the DIG in the northern part has a much lower surface brightness. We have estimated that at least 24% of the Hα emission in NGC 2188 is diffuse. Thus, this result is in agreement with 30 to 55% that have been measured for the Sculptor group galaxies (Ferguson et al. 1996; Hoopes et al. 1996) and the Magellanic Clouds (Kennicutt et al. 1994). The stability of the DIG fraction of the Hα emission from one galaxy to another strongly enforces the idea that the DIG is photoionized. Finally, Rand (1996) used Hα images of nine edge-on galaxies and investigated their halo properties. His work confirmed that DIG in halos of galaxies is correlated with the SFR per unit disk area, or more precisely with $L_{\rm IR}/D_{25}^2$. For NGC 2188 $L_{\rm IR}/D_{25}^2$ is 1.3×10^{40} erg s^{-1} kpc^{-2}, which is comparable to the measured value for NGC 4631 of 1.8×10^{40} erg s^{-1} kpc^{-2}. Since the DIG properties of NGC 2188 are similar to those of NGC 4631, NGC 2188 confirms the picture.

In order to explain the ionization of the DIG at large distances above the plane a picture has been proposed in which OB associations embedded in a low density medium form large Strömgren spheres around them which can even become ionization cones if the ionizing flux is large enough (Miller & Cox 1993; Dove & Shull 1994). The Hα data of NGC 2188 show that the morphology of the ionized gas does not resemble ionization cones but is filamentary instead, with the filaments mostly being oriented perpendicular to the plane. Its structure is reminiscent more of those produced in a superbubble-blowout scenario (e.g. MacLow et al. 1989, Igumentshchev et al. 1990).

5.2. The excitation of the filamentary gas in NGC 2188

The ionization state of the ionized gas in NGC 2188 can be explored using empirical diagnostic diagrams. In these diagrams the emission line ratios of gas that has been ionized by different ionizing sources (e.g. OB star photoionization versus shocks) cover distinct regions.

Fig. 5a-c shows the data in the Baldwin et al. (1981) diagrams as filled squares. Line ratios obtained for LMC HII regions shells are plotted as triangles and for LMC supergiant shells as crosses (Hunter 1994). The solid curve in Fig. 5 represents the empirical location of HII regions defined by Baldwin et al. (1981). The data points for NGC 2188 together with those of the LMC fall along lines somewhat different from those empirical curves. Both galaxies show [NII] λ6584/Hα ratios smaller than those obtained for (mostly) spiral galaxies. In the log([OIII] λ5007/Hβ) versus log([OII]/[OIII]) diagram the line defined by the LMC supergiant shells and the NGC 2188 data is shifted to the upper right, i.e. for the same [OII]/[OIII] we find a higher [OIII] λ5007/Hβ. These shifts can be explained by decreased abundances. The dashed lines in Fig. 5 represent the empirical relationship for lower abundances by Hunter (1994). The LMC as well as the NGC 2188 measurements are well rep-

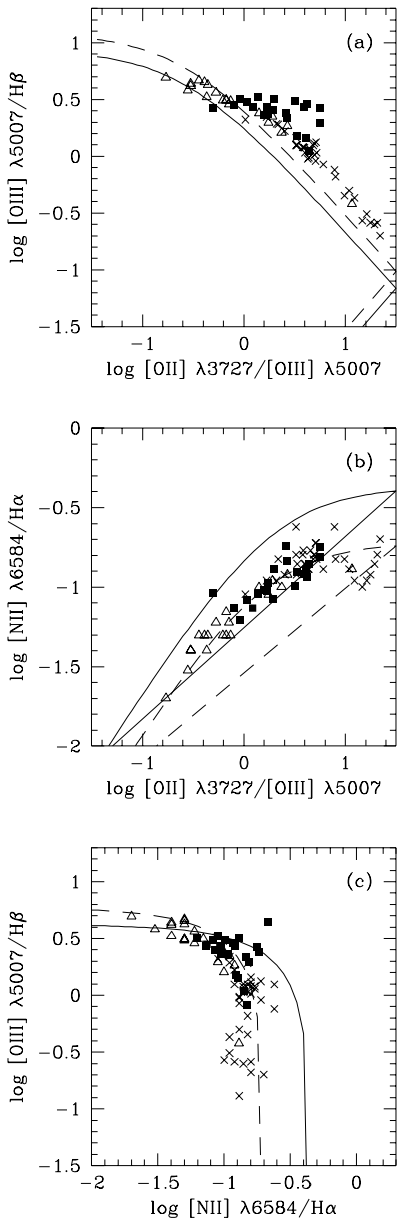

Fig. 5. a The logarithmic intensity ratio of [OIII] λ5007/Hα is plotted against log([OII]/[OIII]). Filled squares represent the line ratios measured for NGC 2188, triangles LMC HII regions, and crosses LMC supergiant shells (Hunter 1994). The solid line is the empirical HII region fit obtained by Baldwin et al (1981), the dashed line is an equivalent relation for lower metallicities obtained by Hunter (1994). **b** The same, but for log([NII] λ6584/Hα) versus log([OII]/[OIII]). **c** The same, but for log([OIII] λ5007/Hβ) versus log([NII] λ6584/Hα).

resented by these curves, implying that the extraplanar Hα emitting gas in NGC 2188 is photoionized.

Theoretically the distribution of the photoionized emission line gas along a line in the diagnostic diagrams comes from a variation of the excitation parameter, $U = \frac{1}{3}\langle n_{ph}/n_e\rangle$, along this line. U basically determines the ionization balance in an HII region. Gas with a low excitation parameter shows strong emission in low ionization species (e.g. N^+, O^+) and is weak in O^{2+}. Fig. 5 shows that the line ratios of LMC supergiant shells occupy regions in the diagram different from those of LMC HII regions. This means that the LMC HII regions have a high excitation parameter whereas that of the ionized shells is much lower. The spectra of NGC 2188 cover HII regions as well as filamentary gas, i.e. gas with a variety of excitation conditions. Still it is found that the line ratios of NGC 2188 cover a much smaller region in the diagnostic diagrams than those of the LMC. They seem to fill the gap between the LMC HII regions and the LMC supergiant shells. One explanation is that the lower spatial resolution of our data due to the larger distance of NGC 2188 leads to a less precise morphological distinction between HII region and extra-HII region filaments. For the low surface brightness emission in NGC 2188 we additionally expect a somewhat higher excitation parameter since we find these filaments to emerge directly from HII regions. Therefore, they likely see a less diluted radiation field than the filaments forming the edges of the supergiant shells in the LMC.

The fact that the ionization of the filamentary emission in NGC 2188 can be explained by a decrease of U is in agreement with results that have been obtained for the DIG in the Galaxy (Mathis 1986, Domgörgen & Mathis 1994). Also Domgörgen & Mathis (1994) predict $He^+/H^+ \sim 0.6$ He/H from their model calculations assuming that the mean spectral type responsible for the ionization of the DIG has a temperature of $T_e = 38,000$ K which is equivalent to an O7 star. The upper limits on He^+/H^+ provided by the data presented here are in agreements with the prediction from the photoionization calculations.

5.3. Comparison with other galaxies

The results obtained will now be compared to line ratios that have been measured for diffuse ionized features in other galaxies. Since NGC 2188 is an irregular galaxy we start out by exploring the properties of its filamentary Hα emitting gas with respect to the so-called "interstellar froth". A comparison with the LMC interstellar froth has already been completed in the last paragraph. What is found for other irregulars? The line ratios of HII regions and ionized filaments in several irregular galaxies have been investigated by Hunter & Gallagher (1990). Their results are equivalent to several of those reported here. Generally the relative intensities of the low ionization states are increased for diffuse features with respect to HII regions. Hunter & Gallagher (1990) find for the HII regions: [SII] λ6717/H$\alpha \sim 0.14$, [NII] λ6584/H$\alpha \sim 0.10$, and [OII]/[OIII] ~ 1.5 and for the filaments [SII] λ6717/H$\alpha \sim 0.23$, [NII] λ6584/H$\alpha \sim 0.15$, and [OII]/[OIII] ~ 3.5, in agreement with our results. We conclude that the nature of the filamentary gas in NGC 2188 is very similar and possibly equivalent to those of the ionized froth in other irregular galaxies.

The variation of the [SII] and [NII] to Hα ratios with vertical distance from the plane has been studied for the edge-on spiral galaxies NGC 4631 (Golla et al. 1996) and NGC 891 (Dettmar & Schulz 1992). Both galaxies show widespread layers of Hα emitting gas in their halos. Investigations of the emission line ratios were restricted to the wavelength regime around

Hα, i.e. to [SII] λ6717/Hα and [NII] λ6584/Hα. Both line ratios increase with vertical distance z from the midplane. For NGC 891 [SII] λ6717/Hα = 0.11 $\pm$ 0.05 and [NII] λ6584/Hα = 0.32 $\pm$ 0.05 in the disk. At z = $\pm$450 pc, the ratios are 0.3 and, 0.6, respectively. At z = $\pm$950 pc, they are 0.6 $\pm$ 0.1 and 1.1 $\pm$ 0.2. In NGC 4631 [SII] λ6717/Hα and [NII] λ6584/Hα are $\sim$ 0.12 in the disk. The highest [SII] and [NII] line ratios are measured for a slit positions parallel to the major axis of the galaxy at $1 - 1.5$ kpc above the midplane and are for both $\sim 0.7 \pm 0.12$.

The results for NGC 2188 are similar to those of NGC 4631 and NGC 891 in that the line ratios of [SII] and [NII] increase with z. It has been suggested that scattering of HII region light by dust might considerably alter the line ratios of the ionized gas also at high z. In this picture a continuous variation of line ratios with z is not intrinsic but inferred by a decreasing contribution of scattered light (Ferrara et al. 1996). Since NGC 2188 is poor in dust the continuous variation of the line ratios with offset from the central HII region peak suggests a different picture. In the last section it was shown that the line ratios of NGC 2188 can be explained by photoionization. The variation of the relative line strength with z is then due to a decreasing excitation parameter. Since the excitation parameter describes the ratio of photon density to electron density an explanation is that the Ly continuum photon density decreases continuously with z.

Next we will compare the absolute line intensity ratios for [NII] λ6584/Hα and [SII] λ6717/Hα. The highest line ratios obtained for the two spirals belong to gas at $z \sim 1$ kpc and $EM \sim 40\,\mathrm{cm}^{-6}$ pc. The gas is thus higher above the midplane and its emission is weaker than the features for which we measured the spectrum. Therefore we compare the extraplanar gas in NGC 2188 to the extraplanar gas $\sim$ 600 pc above the midplane of NGC 891. We then find that [SII] λ6717/Hα is largely similar for all three galaxies, with [SII] λ6717/H$\alpha \sim 0.1$ in the disk and ~ 0.4 for the diffuse emission. However, the differences are pronounced for [NII], with [NII] λ6584/Hα being systematically higher in disk and halo of NGC 4631 and NGC 891. The same discrepancy we find when comparing average line ratios of HII regions and DIG in the Milky Way with those of NGC 2188.

The similarity in [SII] λ6717/Hα and the differences in [NII] λ6584/Hα can be explained in terms of differing N/S abundances. Whereas S is a product of primary nucleosynthesis, N comes from both primary and secondary nucleosynthesis (Pagel 1994). Therefore N/O is smaller in irregular galaxies than it is in spirals whereas S/O is similar for both types of galaxies. A decreased absolute metallicity results in a higher nebular temperature, and thus only S/O and not S/H is important. The low N/O, however, directly affects [NII] λ6584/Hα. This can also be seen in Fig. 5a and b by comparing the empirical HII region fits by Baldwin et al. (1981) with the equivalent relation for lower metallicities by Hunter (1994).

It has been speculated that the enhanced [SII] and [NII] emission of the DIG is due to additional photoelectric heating of the DIG by dust grains (Reynolds & Cox 1992). The data presented here argue against this. NGC 2188 has a dust-to-HI mass ratio which is typical for irregulars but much smaller than for spirals. Therefore photoelectric heating by dust grains, if present, should be less important in NGC 2188 than in NGC 891, NGC 4631, and the Galaxy. However, variation and strength of the [SII] λ6717/Hα intensity ratio in NGC 2188 are comparable to that found in other galaxies and the weakness of [NII] λ6584/Hα can be accounted for by a low N abundance. Thus, heating by dust does not seem to play a significant role for producing the line ratios observed.

Not all the line ratios measured for the DIG can be accounted for by photoionization. In particular the non-detection of He^+ in the Galaxy remains puzzling. Additionally, Fig. 5a und b show that the high [NII] λ6584/Hα of 1.1 measured at 1 kpc above the plane of NGC 891 lies well outside of the HII region regime in the diagnostic diagrams. Possibly heating and ionization mechanisms other than photoionization are important here. In NGC 891 the velocities of the Hα emitting gas above the plane (Pildis et al. 1994), the existence of a radio halo (Allen et al. 1978), and an X-ray halo (Bregman & Pildis 1994) indicate the presence of outflows from the disk into the halo of the galaxy. In that case shocks produced by the outflowing gas could play an important role for the ionization of the DIG in the halo (Heckman et al. 1990). The low [OI]/H$\alpha < 0.05$ is not in contradiction with this interpretation. Another critical indicator for this scenario is the yet unobserved [OIII] λ5007 which would have to increase at high distances above the plane. Evidence for such a scenario has recently been found for the edge-on spiral galaxy NGC 4666 (Dahlem et al. 1996).

6. Summary and conclusions

We investigated the properties of the ionized gas in the dwarf irregular galaxy NGC 2188 using Hα images and optical spectroscopy. NGC 2188 shows spectacular features of ionized gas emerging from a star forming complex into the halo of the galaxy. These filaments are morphologically similar to the extraplanar gas detected in the lower halo of the edge-on spiral NGC 891. Since NGC 2188 is a dust-poor low-metallicity galaxy, the data presented here facilitate the study of properties of extraplanar DIG under conditions different from those typically found in spirals. The following conclusions can be drawn from the data:

- The Hα data of NGC 2188 confirm that the existence of DIG is correlated with star forming regions: its existence is pervasive but the most prominent structures occur in the vicinity of a bright HII region complex. We measure that $> 24\%$ of the Hα emission is diffuse in agreement with earlier findings for other galaxies. This supports the idea that the gas is photoionized.
- The extraplanar filaments in NGC 2188 are photoionized. Their line ratios fall in a region of the Baldwin et al. (1981) empirical diagnostic diagrams typically covered by photoionized gas of low metallicity. Additionally, the upper limits that could be set on He^+/H^+ are in agreement with predictions from photoionization modeling.
- The variations in the line ratios can be explained by a decrease of the Ly continuum photon density with vertical

distance z above the plane, or more generally with distance from the ionizing sources: low ionization stages become stronger and [OIII] λ5007/Hβ becomes weaker with distance from the HII region peaks. This is what is expected for a decreasing excitation parameter of the gas due to a diluted photon field.

– The differences between line ratios measured for the DIG in NGC 891, NGC 4631, the Milky Way, and those presented here can be explained by differences in metallicity.
– NGC 2188 is poor in dust. Still the variations in the spectrum of its ionized gas as well as the absolute line ratios are comparable to those of spiral galaxies. We therefore conclude that dust scattering of HII region emission and photoelectric heating play only a minor role in altering the line spectrum of the DIG.
– If the ionized gas in the halo of galaxies is photoionized the Ly continuum photons of OB stars have to travel large distances through the ISM. The morphology of the ionized gas is filamentary and is reminiscent of the "chimneys" produced by dynamical models of the ISM (Norman & Ikeuchi 1989). This suggests that the mechanical energy input of young stars might play an important role for a full understanding of the DIG. In such a picture of the DIG the high [NII] line ratio at 1 kpc above the plane of NGC 891 could naturally be explained if shock ionization due to outflowing gas plays a role at high distances above the plane.

Acknowledgements. We thank R.J. Reynolds, J.S. Mathis, and K.S. de Boer for their comments on the manuscript. Thanks also to M. Dahlem for his contribution to the data reduction. H.D. was supported by the DFG Graduiertenkolleg Magellansche Wolken.

References

Abbott, D.C. 1982, ApJ 263, 723
Allen, R.J., Baldwin, J.E., Sancisi, R. 1978, A&A 62, 397
Baldwin, J.A., Phillips, M.M., Terlevich, R. 1981, PASP 93, 5
Bregman, J.N., Pildis, R.A. 1994, ApJ 420, 570
Brocklehurst, M. 1971, MNRAS 153, 471
Dahlem, M., Petr, M.G., Lehnert, M.D., Heckman, T.M., Ehle, M. 1996, submitted to A&A
Dettmar, R.-J. 1990, A&A 232, L15
Dettmar, R.-J., Schulz, H. 1992, A&A 254, L25
Domgörgen, H., Mathis, J.S. 1994, ApJ 428, 647
Domgörgen, H., Dahlem, M., Dettmar, R.-J. 1996, A&A 313, 96
Dove, J.B., Shull, J.M. 1994, ApJ 430, 222
Ferguson, A.M.N., Wyse, R.F.G., Gallagher, J.S., III, Hunter, D.A. 1996, AJ 111, 2265
Ferrara, A., Bianchi, S., Dettmar, R.-J., Giovanardi, C. 1996, ApJL 467, L69
Gallagher, J.S., III, Hunter, D.A. 1987, in "Star Formation in Galaxies", ed. C. Persson (NASA Cp-2466), p. 167
Gallagher, J.S., III, Hunter, D.A., Tutokov, V. 1984, ApJ 284, 544
Golla, G., Dettmar, R.-J., Domgörgen, H. 1996, A&A 313, 439
Heckman, T.M., Armus, L., Miley, G.K. 1990, ApJS 74, 833
Hoopes, C.G., Walterbos, R.A.M., Greenawalt, B.E. 1996, AJ 112, 1429
Hunter, D.A. 1994, AJ 107, 565
Hunter, D.A., Gallagher, J.S., III, 1990, ApJ 362, 480
Hunter, D.A., Gallagher, J.S., III, Rice, W.L., Gillett, F.C. 1989, ApJ 336, 152
Igumentshchev, I.V., Shustov, B.M., Tutokov, A.V. 1990, A&A 234, 396
Kennicutt, R.C., Bresolin, F., Bomans, D.J., Bothun, G.D., Thompson, I.B. 1995, AJ 109, 594
Lauberts, A., Valentijn, E.A. 1989, ESO, "The Surface Photometry Catalogue of the ESO-Uppsala Galaxies"
Lonsdale, C.J., Helou, G., Good, J.C., Rice, W. 1985, "Cataloged Galaxies and Quasars Observed in the IRAS Survey" (Pasadena: JPL)
MacLow, M.-M., McCray, R., Norman, M.L. 1989, ApJ 337, 141
Mathis, J.S. 1986, ApJ 301, 423
Melnick J., Dekker H., D'Odorico S., 1989, ESO Operating Manual No. 4
Miller, W.W., III, Cox, D.P. 1993, ApJ 417, 579
Norman, C.A., Ikeuchi, S. 1989, ApJ 345, 372
Oliveira, C. 1994, "Update to the Operating Manual for the B&C Spectrograph on the ESO 1.52m telescope"
Pagel, B.E.J. 1994, in "The Formation and Evolution of Galaxies", eds. C. Muñoz-Tuñón & F.Sánchez, Cambridge University Press
Pildis, R.A., Bregman, J.N., Schombert, J.M. 1994, ApJ 423, 190
Rand, R.J. 1996, ApJ 462, 712
Reynolds, R.J. 1984, ApJ 282, 191
Reynolds, R.J. 1985a, ApJ 294, 256
Reynolds, R.J. 1985b, ApJ 298, L27
Reynolds, R.J. 1989, ApJ 345, 811
Reynolds, R.J., Cox, D.P. 1992, ApJ 400, L33
Reynolds, R.J., Tufte, S.L. 1995, ApJ 439, L17
Thronson, H.A., Telesco, C.M., 1986, ApJ 311, 98
Tüg H., White N.W., Lockwood G.W., 1977, A&A 61, 679
Tüg H., 1977, ESO Messenger # 11
Tully R.B., 1988, "Nearby Galaxies Catalog", Cambridge University Press
Shields, G.A., Searle, L. 1978, ApJ 222, 821
Skillman, E.D. 1985, ApJ 290, 449
Stasinska, G., Comte, G., Vigroux, L. 1986, A&A 154, 352

This article was processed by the author using Springer-Verlag LaTeX A&A style file *L-AA* version 3.